Author Manuscript

Author Manuscript

Author Manuscript

Author Manuscript

HHS Public Access

Author manuscript

Nature. Author manuscript; available in PMC 2012 August 02.

Published in final edited form as:

Nature. ; 482(7383): 98–102. doi:10.1038/nature10814.

Mutations in *Kelch-like 3* and *Cullin 3* cause hypertension and electrolyte abnormalities

Lynn M. Boyden[1], **Murim Choi**[1,*], **Keith A. Choate**[2,*], **Carol J. Nelson-Williams**[1], **Anita Farhi**[1], **Hakan R. Toka**[3], **Irina R. Tikhonova**[4], **Robert Bjornson**[4], **Shrikant M. Mane**[4], **Giacomo Colussi**[5], **Marcel Lebel**[6], **Richard D. Gordon**[7], **Ben A. Semmekrot**[8], **Alain Poujol**[9], **Matti J. Välimäki**[10], **Maria E. De Ferrari**[5], **Sami A. Sanjad**[11], **Michael Gutkin**[12], **Fiona E. Karet**[13], **Joseph R. Tucci**[14], **Jim R. Stockigt**[15], **Kim M. Keppler-Noreuil**[16], **Craig C. Porter**[17], **Sudhir K. Anand**[18], **Margo L. Whiteford**[19], **Ira D. Davis**[20], **Stephanie B. Dewar**[21], **Alberto Bettinelli**[22], **Jeffrey J. Fadrowski**[23], **Craig W. Belsha**[24], **Tracy E. Hunley**[25], **Raoul D. Nelson**[26], **Howard Trachtman**[27], **Trevor R. P. Cole**[28], **Maury Pinsk**[29], **Detlef Bockenhauer**[30], **Mohan Shenoy**[31], **Priya Vaidyanathan**[32], **John W. Foreman**[33], **Majid Rasoulpour**[34], **Farook Thameem**[35], **Hania Z. Al-Shahrouri**[35], **Jai Radhakrishnan**[36], **Ali G. Gharavi**[36], **Beatrice Goilav**[37], and **Richard P. Lifton**[1]

[1]Department of Genetics and Howard Hughes Medical Institute, Yale University School of Medicine, New Haven, Connecticut, USA [2]Department of Dermatology, Yale University School of Medicine, New Haven, Connecticut, USA [3]Renal Division, Brigham and Women's Hospital, Boston, Massachusetts, USA [4]Yale Center for Genome Analysis, Yale University, New Haven, Connecticut, USA [5]Nephrology Unit, Niguarda-Ca' Granda Hospital, Milan, Italy [6]Department of Medicine, Laval University, Québec, Canada [7]Endocrine Hypertension Research Centre, University of Queensland School of Medicine, Brisbane, Australia [8]Department of Pediatrics, Canisius Wilhelmina Hospital, Nijmegen, Netherlands [9]Department of Pediatrics, Pays d'Aix Hospital, Aix-en-Provence, France [10]Division of Endocrinology, Department of Medicine, Helsinki University Central Hospital, Helsinki, Finland [11]Department of Pediatrics and Adolescent Medicine, American University Medical Center, Beirut, Lebanon [12]Hypertension Research Center, University of Medicine and Dentistry of New Jersey, Newark, New Jersey, USA [13]Department of Medical Genetics, University of Cambridge, Cambridge, United Kingdom [14]Division of Endocrinology, Roger Williams Medical Center, Providence, Rhode Island, USA [15]Department of

Users may view, print, copy, download and text and data- mine the content in such documents, for the purposes of academic research, subject always to the full Conditions of use: http://www.nature.com/authors/editorial_policies/license.html#terms

Correspondence and requests for materials should be addressed to R.P.L. (richard.lifton@yale.edu).

*These authors contributed equally to this work.

Supplementary Information is linked to the online version of the paper at www.nature.com/nature.

Author contributions L.M.B., M.C., K.A.C., and R.P.L. designed experiments and analyzed data. L.M.B., C.N.W., and I.R.T. performed experiments. A.F., H.R.T., G.C., M.L., R.D.G., B.A.S., A.P., M.J.V., M.E.D.F., S.A.S., M.G., F.E.K., J.R.T., J.R.S., K.M.K.N., C.C.P., S.K.A., M.L.W., I.D.D., S.B.D., A.B., J.J.F., C.W.B., T.E.H., R.D.N., H.T., T.R.P.C., M.P., D.B., M.S., P.V., J.W.F., M.R., F.T., H.Z.A.S., J.R., A.G.G., and B.G. recruited PHAII subjects and families. R.B. and S.M.M. directed the IT and DNA sequencing infrastructure. L.M.B. and R.P.L. wrote the manuscript.

Reprints and permissions information is available at www.nature.com/reprints.

The authors declare no competing financial interests.

Accession numbers: KLHL3: NCBI accessions NM_017415.2, NP_059111.2; CUL 3: NCBI accessions NM_003590.3, NP_003581.1

Author Manuscript Author Manuscript Author Manuscript Author Manuscript

Endocrinology and Diabetes, Ewen Downie Metabolic Unit, Alfred Hospital, Melbourne, Australia [16]Division of Medical Genetics, Department of Pediatrics, University of Iowa Children's Hospital, Iowa City, Iowa, USA [17]Division of Nephrology, Department of Pediatrics, Medical College of Wisconsin, Milwaukee, Wisconsin, USA [18]Department of Pediatrics, David Geffen School of Medicine at UCLA, Los Angeles, California, USA [19]Duncan Guthrie Institute of Medical Genetics, Royal Hospital for Sick Children, Glasgow, United Kingdom [20]Baxter Healthcare Corporation, McGaw Park, Illinois, USA [21]Department of Pediatrics, University of Pittsburgh School of Medicine, Pittsburgh, Pennsylvania, USA [22]Division of Pediatrics, Mandic Hospital, Merate, Italy [23]Department of Pediatrics, Johns Hopkins School of Medicine, Baltimore, Maryland, USA [24]Division of Nephrology, Department of Pediatrics, Saint Louis University Health Sciences Center, St. Louis, Missouri, USA [25]Division of Nephrology, Department of Pediatrics, Vanderbilt University Medical Center, Nashville, Tennessee, USA [26]Division of Nephrology, Department of Pediatrics, University of Utah, Salt Lake City, Utah, USA [27]Division of Nephrology, Cohen Children's Medical Center of New York, New Hyde Park, New York, USA [28]West Midlands Regional Genetics Service, Birmingham Women's Hospital, Birmingham, United Kingdom [29]Division of Nephrology, Department of Pediatrics, University of Alberta, Edmonton, Canada [30]Renal Unit, University College London Institute of Child Health, London, United Kingdom [31]Department of Nephrology, Royal Manchester Children's Hospital, Manchester, United Kingdom [32]Department of Endocrinology, Children's National Medical Center, Washington, DC, USA [33]Department of Pediatrics, Duke University Medical Center, Durham, North Carolina, USA [34]Division of Nephrology, Connecticut Children's Medical Center, Hartford, Connecticut, USA [35]Division of Nephrology, Department of Medicine, University of Texas Health Science Center, San Antonio, Texas, USA [36]Department of Medicine, Columbia University College of Physicians and Surgeons, New York, New York, USA [37]Division of Nephrology, Children's Hospital at Montefiore, Bronx, New York, USA

Abstract

Hypertension affects one billion people and is a principal reversible risk factor for cardiovascular disease. A rare Mendelian syndrome, pseudohypoaldosteronism type II (PHAII), featuring hypertension, hyperkalemia, and metabolic acidosis, has revealed previously unrecognized physiology orchestrating the balance between renal salt reabsorption versus K^+ and H^+ excretion[1]. We used exome sequencing to identify mutations in *Kelch-like 3* (*KLHL3*) or *Cullin 3* (*CUL3*) in 41 PHAII kindreds. *KLHL3* mutations are either recessive or dominant, while *CUL3* mutations are dominant and predominantly *de novo*. CUL3 and BTB-Kelch proteins such as KLHL3 are components of Cullin/RING E3 ligase complexes (CRLs) that ubiquitinate substrates bound to Kelch propeller domains[2–8]. Dominant *KLHL3* mutations are clustered in short segments within the Kelch propeller and BTB domains implicated in substrate[9] and Cullin[5] binding, respectively. Diverse *CUL3* mutations all result in skipping of exon 9, producing an in-frame deletion. Because dominant *KLHL3* and *CUL3* mutations both phenocopy recessive loss-of-function *KLHL3* mutations, they may abrogate ubiquitination of KLHL3 substrates. Disease features are reversed by thiazide diuretics, which inhibit the Na-Cl cotransporter (NCC) in the distal nephron of the kidney; KLHL3 and CUL3 are expressed in this location, suggesting a mechanistic link between *KLHL3*/*CUL3* mutations, increased Na-Cl reabsorption, and disease pathogenesis. These findings

Author Manuscript Author Manuscript Author Manuscript Author Manuscript

demonstrate the utility of exome sequencing in disease gene identification despite combined complexities of locus heterogeneity, mixed models of transmission, and frequent *de novo* mutation, and establish a fundamental role for KLHL3/CUL3 in blood pressure, K^+, and pH homeostasis.

A small number of genes causing Mendelian forms of hypertension have been identified, establishing the role of increased renal salt reabsorption in its pathogenesis[10–12]. The study of pseudohypoaldosteronism type II (PHAII) has identified a physiologic mechanism that orchestrates activities of diverse electrolyte flux pathways, allowing maximal salt reabsorption in response to aldosterone when angiotensin II (AII) is elevated, as in settings of reduced intravascular volume (hypovolemia), versus maximal potassium secretion in settings of hyperkalemia, in which aldosterone is elevated without changes in AII[1]. The role of WNK kinases in this process was revealed by discovery of their mutation in a small fraction of PHAII kindreds[11]. Dominant gain-of-function mutations in *WNK4* or *WNK1* lead to constitutively increased salt reabsorption in the distal nephron regardless of volume status, resulting in hypertension, and inhibition of K^+ secretion despite marked hyperkalemia[1,11,13–17].

We studied a cohort of 52 PHAII kindreds, including 126 affected subjects with renal hyperkalemia and otherwise normal renal function; hypertension and acidosis were present in 71% and 82%, respectively. There was wide variation in disease severity and age of clinical presentation (Supplementary Figs. 1 and 2). Mutations in *WNK1* or *WNK4* were present in only seven of these kindreds (13%). Those without *WNK* mutations had only 2.0 + 1.4 affected members, complicating mapping efforts.

Exome sequencing of eleven unrelated PHAII index cases without *WNK* mutations was performed. Index cases and affected relatives (five trios and one quartet) were also subjected to genome-wide SNP genotyping. Tabulation of high quality novel protein-altering variants revealed 124 genes with three or more variants, 50 with four or more, and 23 with five. Concurrent analysis of linkage among the multiplex families was used to prioritize loci harboring variants that co-segregated with disease; this identified 28 genes with novel protein-altering variants that co-segregated with disease in two or more multiplex families. This revealed *Kelch-like 3* (*KLHL3*) as a strong candidate, with novel *KLHL3* mutations comprising five alleles in three kindreds, all of which co-segregated with the trait. These include one kindred in which affected members are homozygous for a nonsense mutation (W470X), one in which affected members are compound heterozygotes for two missense mutations (F322C and S410L), and one segregating a heterozygous missense mutation (R528H). As a confirmation of significance, Fisher's exact test was used to compare the prevalence of novel protein-altering variants in all genes in PHAII cases versus 699 control exomes. A single gene, *KLHL3*, showed a burden of mutation that surpassed genome-wide significance ($p = 1.1 \times 10^{-8}$; Supplementary Tables 1–3).

KLHL3 was sequenced in all PHAII index cases, identifying novel mutations in 24 (Fig. 1a–b, Supplementary Figs. 3 and 4). Nearly all are at positions conserved among orthologs (Supplementary Fig. 5). Sixteen kindreds have heterozygous mutations that co-segregate with the trait under a dominant model (lod score 6.9, < −2 under other models). In contrast,

Author Manuscript Author Manuscript Author Manuscript Author Manuscript

eight index cases inherited mutations in both *KLHL3* alleles. In these kindreds, affected members are confined to siblings of index cases who inherited the same two mutations, while unaffected relatives inherited zero or one mutation (lod score 4.3 for a recessive model, < −2 for other models). Recessive transmission has not been previously described for PHAII. Consistent with two modes of transmission, subjects with dominant *KLHL3* mutations had significantly higher serum K^+ levels (6.2 ± 0.6 mM) than heterozgyotes for recessive mutations (4.8 ± 0.6 mM) ($p < 10^{-4}$, Student's t-test; normal range 3.5–5.0 mM). These findings establish that PHAII can be caused by either recessive or dominant *KLHL3* mutations. Importantly, we infer that mutations in dominant kindreds are likely dominant-negative, because they phenocopy the features of recessive disease.

KLHL3 contains an N-terminal BTB domain, a BACK domain, and C-terminal Kelch-like repeats that form a six-bladed β-propeller structure[2,4,5] (Fig. 1c–e). There are over 50 BTB-Kelch genes in humans[4]; their propeller domains bind substrate proteins, promoting substrate ubiquitination via interaction of the BTB domain with Cullin 3 (CUL3), a component of a Cullin/RING E3 ubiquitin ligase (CRL)[3,5,6]. Ubiquitination serves diverse functions, including targeting proteins for proteasomal degradation as well as non-degradative roles such as modulation of protein activity, interaction, and localization[7,8].

While recessive *KLHL3* mutations are distributed throughout the encoded protein, dominant *KLHL3* mutations show striking clustering (Fig. 1c). Nine of sixteen dominant mutations alter one of the last four amino acids of the six 'd-a' loops that connect the outermost ('d') β-strand of one Kelch propeller blade to the innermost ('a') β-strand of the next blade. Two others are in 'b-c' loops. These dominant PHAII mutations lie near the hub of the propeller (Fig. 1d) at or near sites implicated in substrate binding in paralogs[9] (Supplementary Fig. 5). Three other dominant mutations cluster within the BTB domain, at or near sites implicated in Cullin binding in paralogs[5]. We infer that dominant mutations in KLHL3 likely impair binding either to specific substrates or to CUL3.

After accounting for *KLHL3*, *WNK1*, and *WNK4* mutations, 21 PHAII kindreds without mutations remained. We considered *KLHL3's* presumed functional partner, *CUL3* (Fig. 1e), as a potential candidate. Among PHAII exomes, novel heterozygous *CUL3* variants were suggested in two. Sequencing *CUL3* in all index cases identified seventeen with novel heterozygous mutations, all in cases without *KLHL3*, *WNK1* or *WNK4* mutations (Fig. 2a, Supplementary Fig. 6). Eight of these mutations were documented to be *de novo*, providing overwhelming evidence that these mutations are disease-causing. *CUL3* mutations all cluster in sites likely involved in splicing of exon 9, including the intron 8 splice acceptor (n = 4), the intron 9 splice donor (n = 5), the putative intron 8 splice branch site (n = 5), and a putative splice enhancer in exon 9 (n = 3, within a TTGGA[T/A] splice enhancer consensus sequence[18]) (Fig. 2b).

To test the impact of these mutations on splicing, *CUL3* genomic DNA spanning exon 8 to exon 10, containing either wild-type sequence or one of nine PHAII mutations, was cloned and expressed in HEK293 cells, and the spliced RNA products were analyzed. While the wild-type sequence produces a properly spliced product containing all three exons, each of the mutants produces a predominant product that skips exon 9, joining exon 8 to exon 10

Author Manuscript Author Manuscript Author Manuscript Author Manuscript

(Fig. 2c–d). This results in an in-frame 57 amino acid deletion (residues 403–459) in the segment linking the BTB-binding and RING-binding domains of CUL3. The fact that *CUL3* mutations phenocopy recessive *KLHL3* mutations suggests that they abrogate CUL3 function at KLHL3 targets.

As with PHAII caused by *WNK1* and *WNK4* mutations[1], virtually all patients with *KLHL3* and *CUL3* mutations have been treated with thiazide diuretics, inhibitors of the Na-Cl cotransporter NCC, with correction of phenotypic abnormalities. WNK4 regulates the activities of NCC[13,14,16], the epithelial Na^+ channel ENaC[17], and the K^+ channel ROMK[15], and is co-expressed with these proteins in the renal distal convoluted tubule (DCT) and collecting duct (CD)[11,19,20]. Staining mouse kidney sections with specific antibodies demonstrated that KLHL3 is predominantly expressed in DCT and CD, with apical localization in DCT (Fig. 3). CUL3 is ubiquitously expressed and is in all nephron segments, with particularly high expression in the proximal tubule, but also in DCT and CD (Supplementary Fig. 7). These findings are consistent with both proteins playing a role in the regulation of salt and electrolyte homeostasis in the distal nephron.

There are highly significant differences in phenotypic severity among PHAII patients with mutations in different genes (Table 1, Supplementary Figs. 1 and 2, Supplementary Table 4). Subjects with *CUL3* mutations presented at much younger ages than those with mutation in *KLHL3*, *WNK1*, or *WNK4*, and had significantly more severe hyperkalemia and metabolic acidosis and were far more likely to have hypertension before age 18 (others commonly develop hypertension at later ages). The majority of subjects with *CUL3* mutations demonstrated failure to thrive or growth impairment. These observations, in conjunction with the high rate of *CUL3 de novo* mutation, support impairment of reproductive fitness. Among the other mutant loci, there remain significant differences in disease severity (rank order recessive *KLHL3* > dominant *KLHL3* > *WNK4* > *WNK1*).

KLHL3 and *CUL3* mutations account for 79% of kindreds in our cohort. Gene identification of was complicated by the combined effects of locus heterogeneity, two modes of transmission at one locus, and few informative meioses. Many heretofore unsolved Mendelian traits may have similar complexities. Use of control exomes as comparators for analysis of mutation burden may be broadly applicable to discovery of such loci.

The most parsimonious mechanism of *KLHL3* and *CUL3* mutations is that they abrogate ubiquitination of targets normally bound by KLHL3, activity that is required for normal modulation of renal salt, K^+, and H^+ handling in response to physiologic challenge; this speculation will require biochemical verification. The fact that recessive mutations in *KLHL3* cause PHAII without other diverse effects implies either that KLHL3 targets are highly restricted to the renal salt and electrolyte pathway, or that loss of KLHL3 function at other targets can be compensated by other loci. BTB-Kelch/CUL3 CRLs can act as dimers, with two substrate-binding domains capable of engaging the same target molecule[7]. This suggests a potential mechanism to explain dominant-negative effects of *KLHL3* and *CUL3* mutations.

Author Manuscript Author Manuscript Author Manuscript Author Manuscript

CUL3-based CRLs participate in a wide range of critical cellular processes[8] via binding diverse BTB domain-containing proteins[3,5]. *CUL3* mutations affecting all or many of these activities would undoubtedly produce very broad phenotypes. *CUL3* mutations in PHAII merely phenocopy the effects of loss of *KLHL3*, suggesting they selectively abrogate function at KLHL3 targets. The stereotypic consequences of *CUL3* mutations, all deleting 57 amino acids in a region linking the BTB-binding and RING-binding domains, support such a specific effect. Consistent with this possibility, introduction of a flexible linker sequence to this region of CUL1 leaves substrate protein binding and ubiquitin polymerization intact, but nonetheless abolishes ubiquitination of a normal substrate[21].

Thiazide diuretics correct abnormalities in virtually all PHAII subjects; similar correction is seen in a mouse model of PHAII with either thiazides or genetic ablation of NCC[16]. These findings suggest that increased NCC activity is likely to be a common pathogenic mechanism. Co-expression of KLHL3 and CUL3 with NCC in DCT, and evidence that NCC is ubiquitinated[22] is consistent with this notion. ROMK and the H^+ ATPase are respectively required for net renal K^+ secretion[23] and H^+ secretion[24] and are also likely targets, although their activity is expected to be decreased, rather than increased, in PHAII. Another thiazide-sensitive Na-Cl cotransport pathway in the collecting duct has recently been described, suggesting an additional potential target[25]. Whether a KLHL3/CUL3 CRL acts directly or indirectly on these targets, whether they alter delivery of NCC and other targets to, or retrieval from, the plasma membrane, and what upstream pathways regulate this activity is unknown. Similarly, whether KLHL3/CUL3 and WNKs operate within the same or different pathways is presently unknown; it is of interest that segments of NRF2 that interact with the Kelch propeller domain of KEAP1 are highly acidic[9,26], akin to the domain of WNK4 that is mutated in PHAII[11].

These findings demonstrate previously unrecognized roles for KLHL3 and CUL3. Understanding the upstream regulators and downstream targets of KLHL3/CUL3 activity will provide further insight into mechanisms underlying maintenance of blood pressure and electrolyte homeostasis in response to diverse environmental challenges.

Methods summary

A cohort of 52 PHAII kindreds comprising 126 affected subjects was ascertained, characterized, and recruited for study. Index cases of eleven kindreds were chosen for whole exome capture and sequencing, and novel variants were identified. Genes were prioritized for follow-up and subjected to Sanger sequencing of index cases of each kindred. Segregation of rare variants within kindreds was analyzed. KLHL3 and CUL3 were localized in kidney by staining with specific antibodies and immunofluorescence microscopy. Effects of *CUL3* mutations on RNA splicing were studied by analysis of spliced products produced in mammalian cells.

Full Methods and associated references are available in the online version of the paper at www.nature.com/nature.

Author Manuscript Author Manuscript Author Manuscript Author Manuscript

Methods

Study subjects

Index cases were referred for pseudohypoaldosteronism type II (PHAII). Patients and participating family members provided consent to a study protocol approved by the Yale Human Investigation Committee. Control exomes were 699 unrelated subjects of European ancestry without hypertension, sequenced as part of diverse gene discovery projects. Genomic DNA was isolated from venous blood via standard methods.

Exome capture, sequencing and variant calling

Genomic DNA from eleven PHAII index cases and 699 controls was captured on NimbleGen 2.1M human exome arrays (Roche) and sequenced on the Illumina GenomeAnalyzer as previously described[31]. Reads were mapped to the reference genome (hg18) using Maq[32] and genotypes of targeted bases were called with SAMtools[33]. Variants found in dbSNP v130 or 1000 Genomes databases were excluded from further analysis. Remaining variants were considered 'novel' and annotated for impact on the encoded protein, conservation, and expression[31]. Aligned reads were viewed with the Integrative Genomics Viewer[34]. Among PHAII cases, 94.2% of targeted bases were read by 8 or more independent reads; sensitivity and specificity of heterozygous calls were estimated at 93.7% and 99.9% by comparison to Illumina SNP genotyping. Among controls, 94.4% of targeted bases were read by 8 or more independent reads; sensitivity and specificity of heterozygous calls were estimated at 94.5% and 99.8%. Sanger sequencing of 212 novel variants from controls with SAMtools quality score ≥ 100 demonstrated validation in 211 and amplification failure in 1, supporting high specificity of variant calls.

SNP genotyping and linkage analysis

For the eleven PHAII index cases and their affected relatives (five trios and one quartet) genome-wide SNP genotyping was performed using Illumina Human610-Quad BeadChips and GenomeStudio software. Approximately 40K tag SNPs were extracted using Plink[35]. Analysis of linkage was performed using Merlin[36], specifying an autosomal dominant model with no phenocopies. Variants from exome sequencing in regions of the genome that were excluded (lod score < -2) were removed from further analysis, while those that supported linkage were prioritized for further evaluation. In kindreds showing potential recessive transmission of PHAII, SNP genotypes were examined for regions of homozygosity, and linkage was performed specifying an autosomal recessive model.

Sanger sequencing of *KLHL3* and *CUL3*

PCR amplification and Sanger sequencing from genomic DNA was performed using standard methods. Primers were designed with Primer3[37]. Variants identified by exome sequencing were verified. All exons and flanking intronic sequences of *KLHL3* and *CUL3* were sequenced from all PHAII index cases. Previously unidentified mutations were discovered and verified by independent amplification and sequencing. Co-segregation of mutations with disease was determined by sequencing in all available kindred members. *CUL3* exon 9 and its flanking intronic sequence was sequenced in 150 unaffected unrelated

Author Manuscript Author Manuscript Author Manuscript Author Manuscript

controls, none of whom were found to harbor previously unidentified variants. It is noteworthy that because of lower or absent sequence coverage at or near intron-exon junctions, splice donor and acceptor mutations in *CUL3* were suggested in two of the 11 PHAII exomes (SAMtools quality scores 96 and 75) but three branch site mutations were outside the exome sequence and one splice enhancer mutation was poorly covered (SAMtools quality score 3).

Genome-wide assessment of mutation burden

Genes show substantial variation in the prevalence of novel or rare protein-altering variants for biological reasons, including differences in gene size and variation in the proportion of bases that are under purifying selection, and for technical reasons, including difficulties in accurately mapping short sequence reads among closely related paralogs. These factors can limit the ability to directly identify disease loci by simply counting and ranking genes according to the absolute number of such variants, particularly for diseases with substantial locus or model heterogeneity. This gene-to-gene variation can be accounted for by use of control exome data. The prevalence of rare variation in each gene in case exomes was compared to the corresponding prevalence in a large set of control exomes with a Fisher's exact test. Variants included in the analysis were protein-altering (missense, nonsense, and splice site mutations) and high quality (≥ 8 independent reads and SAMtools quality score ≥ 100). For a gene-wise test of rare variant burden in a genome with ~21,000 genes, correction for multiple testing suggests a threshold p-value of $\sim 2.4 \times 10^{-6}$, anticipated to produce a false discovery rate (FDR) of one gene per twenty experiments. The false discovery rate of the Fisher's test was evaluated by Monte Carlo simulation, which confirmed an FDR < 1 gene per 20 experiments (Supplementary Table 1). The power to identify trait-related loci was estimated as a function of the number of variants detected in cases and the number of case exomes sequenced (Supplementary Table 2), and the test was applied comparing the eleven PHAII and 699 control exomes (Supplementary Table 3).

Ortholog and paralog comparisons

Protein sequences of orthologs and paralogs were aligned with Clustal W[38]. Crystal structures were examined with Cn3D[39]. The locations of KLHL3 propeller mutations were compared to the crystal structure of human KLHL2 (PDB ID: 2XN4)[27], the closest human paralog[3] (85% amino acid identity in the propeller). The location of the peptide encoded by CUL3 exon 9 was approximated by comparison to the crystal structure of human CUL1 (PDB IDs: 1LDJ, 1LDK)[22,27].

Splicing assay

A 3782 bp segment of *CUL3*, extending from 287 bp proximal to exon 8 to 327 bp distal to exon 10, was amplified by PCR (Advantage 2 polymerase, Clontech) from genomic DNA of nine PHAII patients with different *CUL3* mutations and one subject with wild-type *CUL3* sequence. Products were cloned into the **pcDNA6.2/GW/D-TOPO** mammalian expression vector (Invitrogen), and plasmids were purified (QIAprep, Qiagen) and sequenced. HEK293 cells were transfected independently with each plasmid using Lipofectamine 2000 (Invitrogen) and harvested ~24 hours post-transfection. RNA was isolated using RNeasy

Author Manuscript Author Manuscript Author Manuscript Author Manuscript

with DNase on-column digestion (Qiagen). The spliced expression products were assessed by reverse transcription with oligo(dT) priming (Superscript III RT, Invitrogen) followed by PCR with vector-specific and *CUL3*-specific primers. Products were fractionated and visualized via agarose gel electrophoresis, and sequenced. Untransfected and water controls were negative.

Immunofluorescence

Fresh frozen mouse kidney sections were fixed with ethanol at 4°C for 30 minutes and acetone at −20°C for three minutes, washed with 1X PBS, and permeabilized with 0.1% Triton X-100 (Sigma) at room temperature for ten minutes. Sections were blocked with 10% donkey serum and 1% bovine serum albumin at room temperature for one hour, incubated with primary antibodies at room temperature for one hour or 4°C overnight, washed four times with 1X PBS, incubated with secondary antibody at room temperature for one hour, and washed four times with 1X PBS, with DAPI nuclear counterstain in the second wash. Slides were mounted with Mowiol (Polysciences) and 1% n-propyl gallate (Sigma) as an anti-fade agent. Primary antibodies included 1:100 rabbit anti-KLHL3, 1:50 rabbit anti-CUL3, 1:800 or 1:1200 guinea pig anti-TRPM6 (ab66655, ab1871, and ab47017; Abcam) and 1:400 or 1:800 goat anti-AQP2 (sc-9882, Santa Cruz Biotechnology). Secondary antibodies, diluted 1:800, included donkey Cy3 anti-rabbit, Cy2 anti-guinea pig, and 649 anti-goat IgG (AffiniPure, Jackson Immunoresearch). Staining with secondary antibodies only was consistently negative.

Supplementary Material

Refer to Web version on PubMed Central for supplementary material.

Acknowledgments

We thank the PHAII subjects, their families, and health care professionals whose participation made this study possible; S. Umlauf and the staff of the Yale Center for Genome Analysis; J. Santosuosso; H. Tirrell and the staff of Beckman Coulter Genomics; V. Klump, Y. Lu, U. Scholl, and J. Zhou for providing reagents; W. Hill for artistic assistance with Fig. 1d; and E. Boyden, S. Boyden, L. Cooley, and M. Hochstrasser for helpful discussions. Supported in part by the Leducq Transatlantic Network on Hypertension.

References

1. Kahle KT, Ring AM, Lifton RP. Molecular physiology of the WNK kinases. Annu Rev Physiol. 2008; 70:329–355.10.1146/annurev.physiol.70.113006.100651 [PubMed: 17961084]
2. Lai F, et al. Molecular characterization of KLHL3, a human homologue of the Drosophila kelch gene. Genomics. 2000; 66:65–75.10.1006/geno.2000.6181 [PubMed: 10843806]
3. Furukawa M, He YJ, Borchers C, Xiong Y. Targeting of protein ubiquitination by BTB-Cullin 3-Roc1 ubiquitin ligases. Nat Cell Biol. 2003; 5:1001–1007.10.1038/ncb1056 [PubMed: 14528312]
4. Prag S, Adams JC. Molecular phylogeny of the kelch-repeat superfamily reveals an expansion of BTB/kelch proteins in animals. BMC Bioinformatics. 2003; 4:42.10.1186/1471-2105-4-42 [PubMed: 13678422]
5. Stogios PJ, Downs GS, Jauhal JJ, Nandra SK, Prive GG. Sequence and structural analysis of BTB domain proteins. Genome Biol. 2005; 6:R82.10.1186/gb-2005-6-10-r82 [PubMed: 16207353]
6. Hudson AM, Cooley L. Phylogenetic, structural and functional relationships between WD- and Kelch-repeat proteins. Subcell Biochem. 2008; 48:6–19.10.1007/978-0-387-09595-0_2 [PubMed: 18925367]

Author Manuscript Author Manuscript Author Manuscript Author Manuscript

7. Zimmerman ES, Schulman BA, Zheng N. Structural assembly of cullin-RING ubiquitin ligase complexes. Curr Opin Struct Biol. 2010; 20:714–721.10.1016/j.sbi.2010.08.010 [PubMed: 20880695]
8. Sarikas A, Hartmann T, Pan ZQ. The cullin protein family. Genome Biol. 2011; 12:220.10.1186/gb-2011-12-4-220 [PubMed: 21554755]
9. Lo SC, Li X, Henzl MT, Beamer LJ, Hannink M. Structure of the Keap1:Nrf2 interface provides mechanistic insight into Nrf2 signaling. EMBO J. 2006; 25:3605–3617.10.1038/sj.emboj.7601243 [PubMed: 16888629]
10. Lifton RP, Gharavi AG, Geller DS. Molecular mechanisms of human hypertension. Cell. 2001; 104:545–556. [PubMed: 11239411]
11. Wilson FH, et al. Human hypertension caused by mutations in WNK kinases. Science. 2001; 293:1107–1112.10.1126/science.1062844 [PubMed: 11498583]
12. Choi M, et al. K+ channel mutations in adrenal aldosterone-producing adenomas and hereditary hypertension. Science. 2011; 331:768–772.10.1126/science.1198785 [PubMed: 21311022]
13. Wilson FH, et al. Molecular pathogenesis of inherited hypertension with hyperkalemia: the Na-Cl cotransporter is inhibited by wild-type but not mutant WNK4. Proc Natl Acad Sci U S A. 2003; 100:680–684.10.1073/pnas.242735399 [PubMed: 12515852]
14. Yang CL, Angell J, Mitchell R, Ellison DH. WNK kinases regulate thiazide-sensitive Na-Cl cotransport. J Clin Invest. 2003; 111:1039–1045.10.1172/jci17443 [PubMed: 12671053]
15. Kahle KT, et al. WNK4 regulates the balance between renal NaCl reabsorption and K+ secretion. Nat Genet. 2003; 35:372–376.10.1038/ng1271 [PubMed: 14608358]
16. Lalioti MD, et al. Wnk4 controls blood pressure and potassium homeostasis via regulation of mass and activity of the distal convoluted tubule. Nat Genet. 2006; 38:1124–1132.10.1038/ng1877 [PubMed: 16964266]
17. Ring AM, et al. WNK4 regulates activity of the epithelial Na+ channel in vitro and in vivo. Proc Natl Acad Sci U S A. 2007; 104:4020–4024.10.1073/pnas.0611727104 [PubMed: 17360470]
18. Fairbrother WG, Yeh RF, Sharp PA, Burge CB. Predictive identification of exonic splicing enhancers in human genes. Science. 2002; 297:1007–1013.10.1126/science.1073774 [PubMed: 12114529]
19. Bachmann S, Bostanjoglo M, Schmitt R, Ellison DH. Sodium transport-related proteins in the mammalian distal nephron - distribution, ontogeny and functional aspects. Anat Embryol (Berl). 1999; 200:447–468. [PubMed: 10526014]
20. Welling PA, Ho K. A comprehensive guide to the ROMK potassium channel: form and function in health and disease. Am J Physiol Renal Physiol. 2009; 297:F849–863.10.1152/ajprenal.00181.2009 [PubMed: 19458126]
21. Zheng N, et al. Structure of the Cul1-Rbx1-Skp1-F boxSkp2 SCF ubiquitin ligase complex. Nature. 2002; 416:703–709.10.1038/416703a [PubMed: 11961546]
22. Ko B, et al. RasGRP1 stimulation enhances ubiquitination and endocytosis of the sodium-chloride cotransporter. Am J Physiol Renal Physiol. 2010; 299:F300–309.10.1152/ajprenal.00441.2009 [PubMed: 20392800]
23. Simon DB, et al. Genetic heterogeneity of Bartter's syndrome revealed by mutations in the K+ channel, ROMK. Nat Genet. 1996; 14:152–156.10.1038/ng1096-152 [PubMed: 8841184]
24. Karet FE, et al. Mutations in the gene encoding B1 subunit of H+-ATPase cause renal tubular acidosis with sensorineural deafness. Nat Genet. 1999; 21:84–90.10.1038/5022 [PubMed: 9916796]
25. Leviel F, et al. The Na+-dependent chloride-bicarbonate exchanger SLC4A8 mediates an electroneutral Na+ reabsorption process in the renal cortical collecting ducts of mice. J Clin Invest. 2010; 120:1627–1635.10.1172/jci40145 [PubMed: 20389022]
26. Tong KI, et al. Different electrostatic potentials define ETGE and DLG motifs as hinge and latch in oxidative stress response. Mol Cell Biol. 2007; 27:7511–7521.10.1128/mcb.00753-07 [PubMed: 17785452]
27. Wang Y, et al. MMDB: annotating protein sequences with Entrez's 3D-structure database. Nucleic Acids Res. 2007; 35:D298–300.10.1093/nar/gkl952 [PubMed: 17135201]

Author Manuscript Author Manuscript Author Manuscript Author Manuscript

28. Zhang MQ. Statistical features of human exons and their flanking regions. Hum Mol Genet. 1998; 7:919–932. [PubMed: 9536098]

29. Voets T, et al. TRPM6 forms the Mg2+ influx channel involved in intestinal and renal Mg2+ absorption. J Biol Chem. 2004; 279:19–25.10.1074/jbc.M311201200 [PubMed: 14576148]

30. Fushimi K, et al. Cloning and expression of apical membrane water channel of rat kidney collecting tubule. Nature. 1993; 361:549–552.10.1038/361549a0 [PubMed: 8429910]

31. Choi M, et al. Genetic diagnosis by whole exome capture and massively parallel DNA sequencing. Proc Natl Acad Sci U S A. 2009; 106:19096–19101.10.1073/pnas.0910672106 [PubMed: 19861545]

32. Li H, Ruan J, Durbin R. Mapping short DNA sequencing reads and calling variants using mapping quality scores. Genome Res. 2008; 18:1851–1858.10.1101/gr.078212.108 [PubMed: 18714091]

33. Li H, et al. The Sequence Alignment/Map format and SAMtools. Bioinformatics. 2009; 25:2078–2079.10.1093/bioinformatics/btp352 [PubMed: 19505943]

34. Robinson JT, et al. Integrative genomics viewer. Nat Biotechnol. 2011; 29:24–26.10.1038/nbt.1754 [PubMed: 21221095]

35. Purcell S, et al. PLINK: a tool set for whole-genome association and population-based linkage analyses. Am J Hum Genet. 2007; 81:559–575.10.1086/519795 [PubMed: 17701901]

36. Abecasis GR, Cherny SS, Cookson WO, Cardon LR. Merlin--rapid analysis of dense genetic maps using sparse gene flow trees. Nat Genet. 2002; 30:97–101.10.1038/ng786 [PubMed: 11731797]

37. Rozen S, Skaletsky H. Primer3 on the WWW for general users and for biologist programmers. Methods Mol Biol. 2000; 132:365–386. [PubMed: 10547847]

38. Larkin MA, et al. Clustal W and Clustal X version 2.0. Bioinformatics. 2007; 23:2947–2948.10.1093/bioinformatics/btm404 [PubMed: 17846036]

39. Wang Y, Geer LY, Chappey C, Kans JA, Bryant SH. Cn3D: sequence and structure views for Entrez. Trends Biochem Sci. 2000; 25:300–302. [PubMed: 10838572]

Author Manuscript Author Manuscript Author Manuscript Author Manuscript

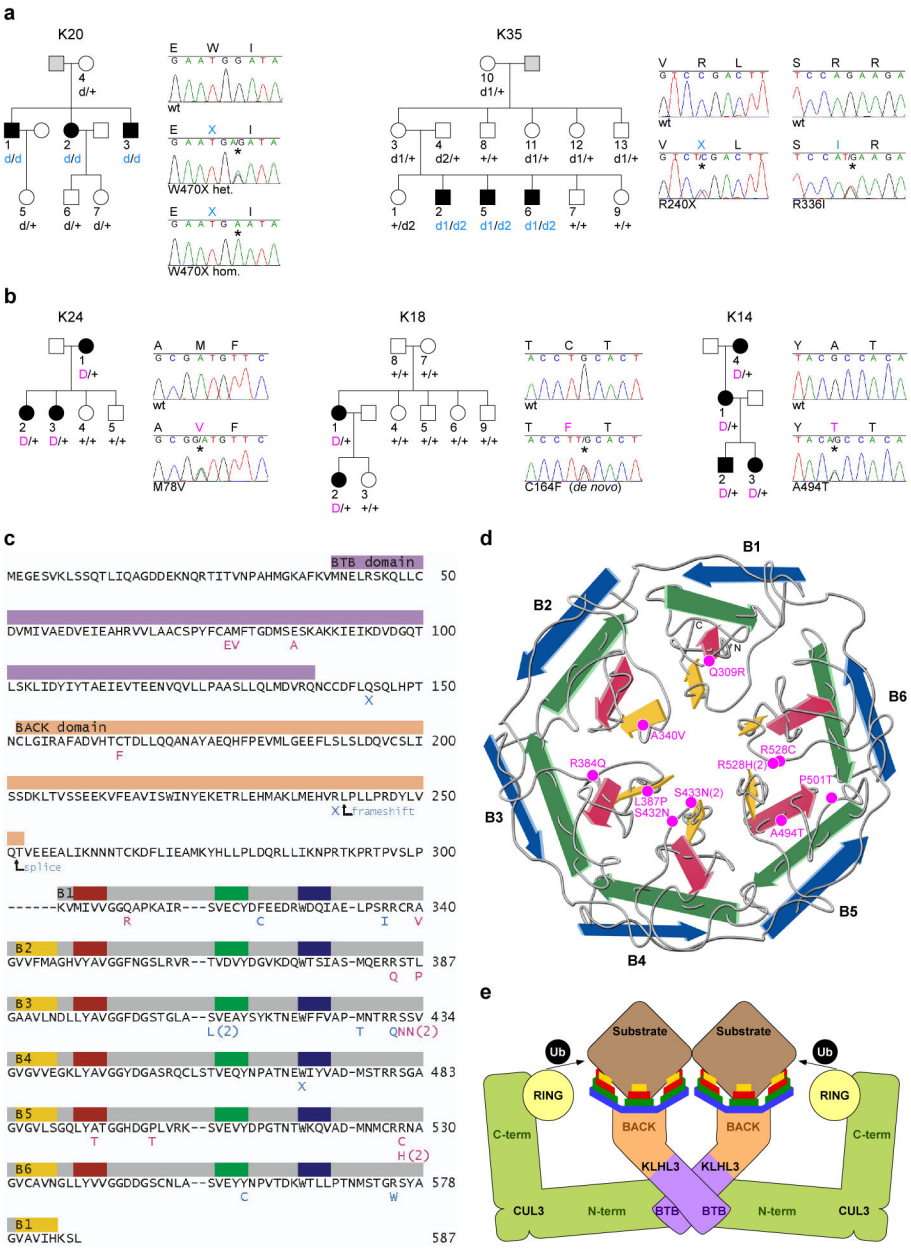

Figure 1. Recessive and dominant *KLHL3* mutations in PHAII kindreds

a–b, Representative kindreds demonstrating recessive (**a**) and dominant (**b**) *KLHL3* mutations (all 24 kindreds are shown in Supplementary Figs. 3–4). Affected, unaffected, and phenotype-undetermined subjects are denoted by black, white, and gray symbols, respectively. *KLHL3* alleles are denoted by '+' (wild-type), 'd' (recessive mutation), and 'D' (dominant mutation). Sequence traces show wild-type (wt) and mutant (*) alleles and encoded amino acids. **c**, KLHL3 protein sequence. Colored bars indicate BTB domain (lavender), BACK domain (peach), and Kelch propeller blades (B1-B6, gray) with β-strands 'a'–'d' in yellow, red, green, and blue respectively. Recessive (aqua) and dominant (pink) mutations are shown; recurrences indicated by numbers. **d**, Kelch propeller schematic, from

KLHL2 crystal structure[27]. β-strands colored as in **c**; dominant mutations indicated. **e**, CRL schematic, comprising a BTB-Kelch protein (KLHL3), CUL3, and a ubiquitin transfer-mediating RING protein, with substrate bound via the Kelch propeller. Complex shown as a dimer[7].

Author Manuscript Author Manuscript Author Manuscript Author Manuscript

Author Manuscript Author Manuscript Author Manuscript Author Manuscript

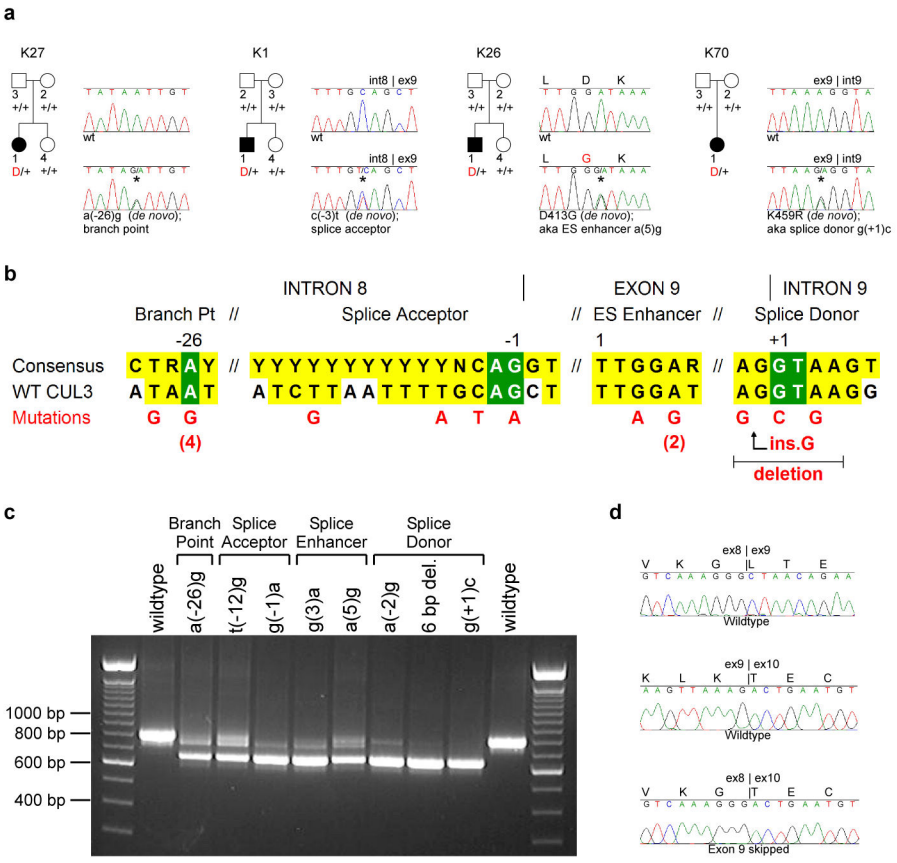

Figure 2. Dominant *CUL3* mutations in PHAII kindreds cause skipping of exon 9

a, Representative kindreds demonstrating *CUL3* mutations, depicted as in Fig. 1 (all 17 kindreds are shown in Supplementary Fig. 6). **b**, *CUL3* mutation locations. Consensus splicing sequences[18,28] and corresponding wildtype *CUL3* sequences within intron 8, exon 9, and intron 9 are shown; invariant bases (green) and consensus homology (yellow) are indicated. Positions numbered relative to splice sites and first base of the exonic splice (ES) enhancer. Mutations shown in red; recurrences indicated by numbers. **c**, RT-PCR of spliced RNA. Wild-type *CUL3* constructs produce a single product including exons 8, 9, and 10 (844 bp); all nine mutants tested produce a predominant product that skips exon 9 (673 bp). **d**, Representative RT-PCR sequences. Wild-type construct produces cDNA with properly spliced junctions between exons 8–9 (top) and 9–10 (middle), while mutant construct [splice donor g(+1)c] produces cDNA joining exon 8 to exon 10 (bottom).

Author Manuscript Author Manuscript Author Manuscript Author Manuscript

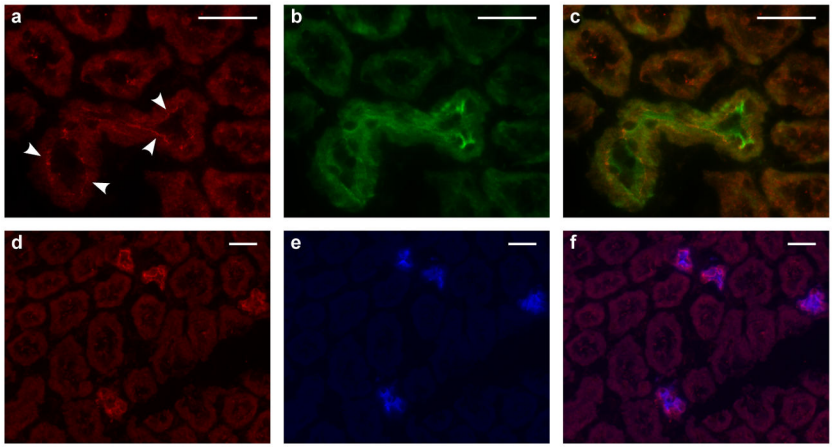

Figure 3. *KLHL3* expression in the kidney

Mouse kidney sections stained with antibodies to KLHL3 (red), TRPM6 (a marker of the DCT[29], green) and AQP2 (a marker of the CD[30], blue). Scale bars 25 μm. **a**–**c**, Staining for KLHL3 (**a**), TRPM6 (**b**), and the merged image (**c**) demonstrates KLHL3 expression in the DCT with apical localization (arrowheads). **d**–**f**, Staining for KLHL3 (**d**), AQP2 (**e**), and the merged image (**f**) demonstrates KLHL3 expression in CD.

Author Manuscript Author Manuscript Author Manuscript Author Manuscript

Table 1

PHAII phenotypes, stratified by genotype.

Mutant Gene	# Kindreds	# Affecteds	Dx/Ref Age	K^+ (mM) (nl 3.5–5.0)	HCO_3^- (mM) (nl 22–28)	% htn ≤age 18
CUL3	17	21	9 ±6	7.5 ±0.9	15.5 ±2.0	94
KLHL3 Recessive	8	14	26 ±14	6.8 ±0.5	17.6 ±1.5	14
KLHL3 Dominant	16	40	24 ±18	6.2 ±0.6	17.2 ±2.5	17
WNK4	5	15	28 ±18	6.4 ±0.7	20.8 ±2.3	10
WNK1	2	23	36 ±20	5.8 ±0.8	22.4 ±4.6	13
			p = 0.0002	p < 0.0001	p < 0.0001	p < 0.0001

Dx/Ref Age, age at diagnosis or referral; K^+, serum potassium; HCO_3^-, serum bicarbonate; % htn ≤age 18, % affecteds diagnosed with hypertension by age 18; nl, normal range. Values for Dx/Ref Age, K^+, and HCO_3^- are means ± standard deviations. Significance of differences among genotype classes was calculated by ANOVA (Dx/Ref Age, K^+, HCO_3^-) or Fisher's exact test (% htn ≤18).

Nature. Author manuscript; available in PMC 2012 August 02.